

Characteristics of Alfvén eigenmodes, burst modes and chirping modes in the Alfvén frequency range driven by negative ion based neutral beam injection in JT-60U

To cite this article: Y. Kusama *et al* 1999 *Nucl. Fusion* **39** 1837

View the [article online](#) for updates and enhancements.

You may also like

- [Simultaneous measurements of unstable and stable Alfvén eigenmodes in JET](#)
R.A. Tinguely, J. Gonzalez-Martin, P.G. Puglia et al.
- [Energetic particles in spherical tokamak plasmas](#)
K G McClements and E D Fredrickson
- [Energetic particle physics in fusion research in preparation for burning plasma experiments](#)
N.N. Gorelenkov, S.D. Pinches and K. Toi

Characteristics of Alfvén eigenmodes, burst modes and chirping modes in the Alfvén frequency range driven by negative ion based neutral beam injection in JT-60U

Y. Kusama, G.J. Kramer, H. Kimura, M. Saigusa^a, T. Ozeki, K. Tobita, T. Oikawa, K. Shinohara, T. Kondoh, M. Moriyama, F.V. Tchernychev^b, M. Nemoto, A. Morioka, M. Iwase, N. Isei, T. Fujita, S. Takeji, M. Kuriyama
Naka Fusion Research Establishment,
Japan Atomic Energy Research Institute,
Naka-machi, Naka-gun, Ibaraki-ken, Japan

R. Nazikian, G.Y. Fu, K.W. Hill, C.Z. Cheng
Princeton Plasma Physics Laboratory,
Princeton University,
Princeton, New Jersey,
United States of America

Abstract. The excitation and stabilization of Alfvén eigenmodes and their impact on energetic ion confinement were investigated with negative ion based neutral beam injection at 330–360 keV into weak or reversed magnetic shear plasmas on JT-60U. Toroidicity induced Alfvén eigenmodes (TAEs) were observed in weak shear plasmas with $\langle\beta_h\rangle \geq 0.1\%$ and $0.4 \leq v_{b\parallel}/v_A \leq 1$. The stability of TAEs is consistent with predictions by the NOVA-K code. New burst modes and chirping modes were observed in the higher β regime of $\langle\beta_h\rangle \geq 0.2\%$. The effect of TAEs, burst modes and chirping modes on fast ion confinement has been found to be small so far. It was found that a strongly reversed shear plasma with internal transport barrier suppresses AEs.

1. Introduction

The weak or reversed magnetic shear configuration is important for advanced tokamak operation because the safety factor profile (q profile) having a weak or reversed shear region is compatible with a hollow current density profile formed by high bootstrap current [1]. However, a great uncertainty is collective energetic particle effects in advanced tokamak modes. In particular, toroidicity induced Alfvén eigenmodes (TAEs) have the lowest damping [2–4]. The stability of AEs depends strongly on the q profile [5, 6]. Alpha particle driven TAEs were actually observed for central alpha particle β as low as $\beta_\alpha \approx 0.02\%$ in weak shear DT plasmas on TFTR [7, 8]. In the ion cyclotron range of frequency (ICRF) heating of JT-60U reversed shear plasmas, TAEs were stable for strongly reversed shear plasmas with a steep density gradient formed by the internal transport barrier (ITB) [9, 10].

^a *Present address:* Ibaraki University, Nakanarusawa 4-12-1, Hitachi-shi, Ibaraki-ken 316-0033, Japan.

^b *Present address:* A.F. Ioffe Physical–Technical Institute, Politechnicheskaya 26, St. Petersburg, Russian Federation.

On JT-60U, negative ion based neutral beams (NNBs: ≤ 500 keV, ≤ 10 MW) [11, 12] can produce a peaked profile of fast ions and a high fast ion β of $\sim 1\%$. Furthermore, JT-60U has a capability to control shaping and q profile using reversed shear operation [13–15]. AEs have been investigated intensively in recent experiments involving NNB injection into weak or reversed shear plasmas to suppress AEs in advanced tokamak modes. This article presents the results. The Alfvén eigenmodes experiment with NNBs is summarized in Section 2, the NNB driven TAEs are described in Section 3, burst and chirping modes excited with NNBs are discussed in Section 4, stabilization of TAEs in strongly reversed shear plasmas is presented in Section 5 and Section 6 summarizes the article.

2. Alfvén eigenmodes experiment with NNBs

The plasma configuration used in this series of experiments and two NNB beam lines are shown in Fig. 1. The toroidal magnetic field was selected to be 1.2–1.7 T for weak shear discharges and 2.1 T

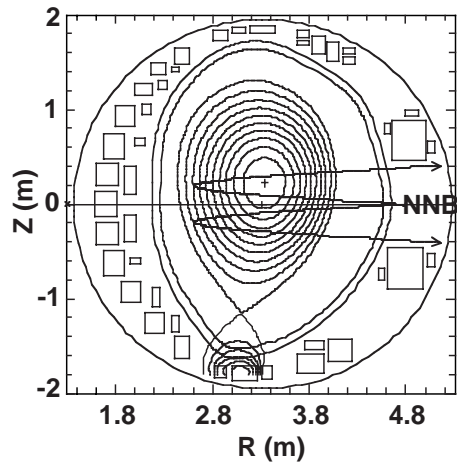


Figure 1. Plasma configuration and two beam lines of NNBs.

for reversed shear discharges. The low field operation can increase the ratio $v_{b\parallel}/v_A$, which is one of the important parameters for TAE excitation. Here, $v_{b\parallel} = v_b(R_{tan}/R_p)$ is the beam ion velocity in the direction of the toroidal magnetic field estimated at the magnetic axis (v_b is the injection velocity of the NNB, $R_{tan} = 2.6$ m is the tangency radius of the NNB and R_p is the major radius of the plasma) and $v_A \propto B_{t0}/(2\bar{n}_e)^{1/2}$ is the Alfvén velocity (B_{t0} is the toroidal magnetic field on the magnetic axis and \bar{n}_e is the line averaged electron density). The ratio $v_{b\parallel}/v_A$ could be increased to 0.95 by increasing electron density. The safety factor at the plasma surface was in the range 4.7–5.5. In this series of experiments, an NNB of 2–4 MW was injected at 330–360 keV into deuterium or helium plasmas. The volume averaged fast ion β , $\langle\beta_h\rangle$, increased to $\sim 0.6\%$ and the fast ion β in the core region increased to $\sim 2\%$. In Fig. 1, the upper beam line passes near the centre of the plasma and the lower beam line is shifted ~ 0.3 m from the centre. By selecting one of two beam lines, the pressure profile of NNB ions can be modified. The q profile, which is indispensable for AE studies, was measured with motional Stark effect (MSE) spectroscopy [16].

3. Toroidal Alfvén eigenmodes

Figure 2 shows the TAEs observed during NNB injection. Time traces of plasma current I_p , line averaged electron density \bar{n}_e and NNB power P_{NNB} are shown in the top part of the figure. An NNB of 1.5–2 MW was injected at 360 keV into a helium plasma

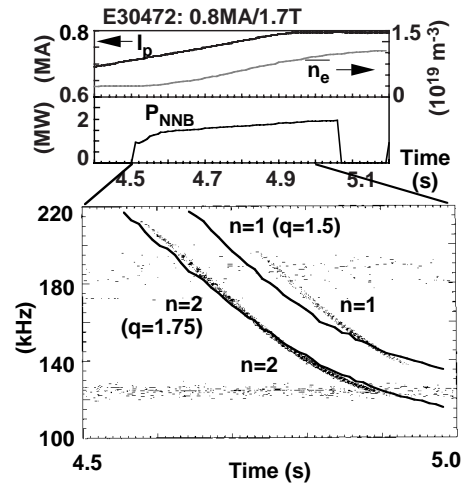


Figure 2. NNB driven TAEs with toroidal mode numbers $n = 1$ and $n = 2$. A H^0 NNB was injected at 360 keV into a helium plasma. Top: time traces of plasma current I_p , line averaged electron density \bar{n}_e and NNB power P_{NNB} . $B_{t0} = 1.7$ T and $I_p = 0.8$ MA at a flat-top. Bottom: TAE frequencies calculated with \bar{n}_e and B_{t0} are shown with solid curves. Here, $q = 1.5$ for the $n = 1$ mode and $q = 1.75$ for the $n = 2$ mode were assumed.

during the current ramp-up. The sawtooth could not be observed during the NNB injection, which showed that the safety factor at the centre was higher than unity. As shown on a frequency spectrum of magnetic fluctuations in the bottom part of the figure, TAEs with toroidal mode numbers $n = 1$ and $n = 2$ were observed. The $n = 2$ mode appears first and the $n = 1$ mode follows. Solid curves in the frequency spectrum show the TAE frequency calculated with \bar{n}_e and B_{t0} ($f_{TAE} \propto B_{t0}/(2\bar{n}_e)^{1/2}$). The measured mode frequency can be well explained by assuming a safety factor q of 1.5 for the $n = 1$ mode and 1.75 for the $n = 2$ mode. The ratio $v_{b\parallel}/v_A$ is in the range 0.4–0.7 during the appearance of TAEs. Using the orbit following Monte Carlo (OFMC) code [17], $\langle\beta_h\rangle$ was evaluated to be $\sim 0.09\%$. This value is comparable to the threshold β_α in weak shear DT discharges on TFTR [7, 8] and is about one fifth to one tenth the threshold value for excitation of TAEs with tangential neutral beams in TFTR [4] and DIII-D [18, 19] positive shear plasmas. TAEs disappear before the turn-off of the NNB and the TAE is stable for later beam injection. In Fig. 2, TAEs persist for 0.2–0.35 s, in contrast to burst TAEs lasting a few milliseconds in TFTR [4] and DIII-D [20]. In the case of Fig. 2, the TAE amplitude is saturated at $\tilde{B}/B \approx 10^{-8}$ at the Mirnov coil location. The saturation is

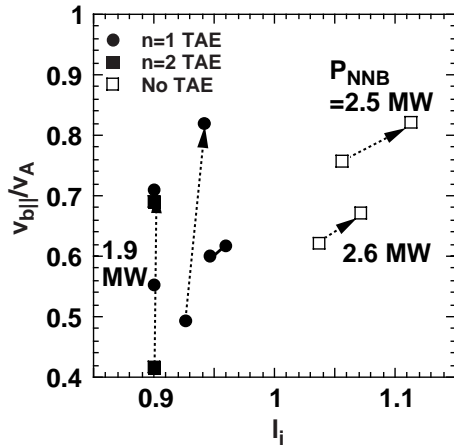


Figure 3. A domain of TAE excitation for H^0 NNB injection into helium plasmas is shown in a plot of $v_{b||}/v_A$ versus internal inductance ℓ_i .

considered to be due to the small fast ion drive by low fast ion β .

Figure 3 shows a domain of TAE excitation in a plot of $v_{b||}/v_A$ versus the internal inductance ℓ_i ($= 2(\Lambda - \beta_p)$) for H^0 NNB injection into helium plasmas. Full circles and squares represent $n = 1$ mode and $n = 2$ mode excitation, respectively; open squares indicate cases without TAE excitation. The NNB power and line averaged electron density were 1.9–2.6 MW and $(0.28\text{--}0.89) \times 10^{19} \text{ m}^{-3}$, respectively. It is indicated that the $n = 1$ and $n = 2$ TAEs are unstable for $\ell_i \leq 1$ and that the TAE is stable for $\ell_i \geq 1$ even for higher NNB powers. A magnetic shear effect or the misalignment of TAE gaps with the high pressure gradient region of fast ions, or both are considered to be the stabilizing mechanism. Figure 4(a) shows the Alfvén continuum spectrum for the $n = 2$ mode calculated using the NOVA-K code and the q profile with $q_0 \approx 1.4$ at 4.8 s in the discharge presented in Fig. 2. The measured TAE frequency is represented by a dashed line. The figure shows that the TAE gap is well aligned over the minor radius and the TAE is considered to be excited in the gap located at $r/a \approx 0.6$. The TAE gap is well aligned also for the $n = 1$ mode and the location of the gap is at $r/a \approx 0.3$. The gap locations of the $n = 1$ and $n = 2$ modes coincide with the region where a large pressure gradient of NNB ions is formed on the fast ion pressure profile, and $\omega_{*h} \geq \omega_{TAE}/2$, which is the necessary condition for TAE excitation, is satisfied (ω_{*h} is the diamagnetic drift frequency of fast ions).

In order to test the effect of decreasing q_0 on TAE stability, the Alfvén continuum spectrum was

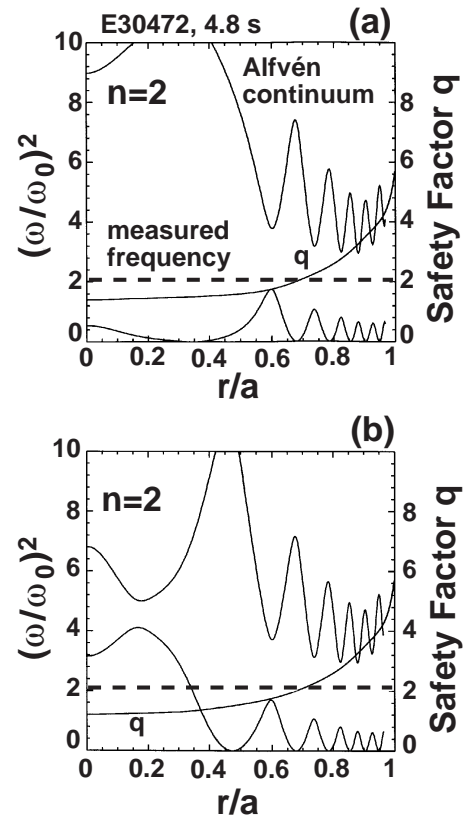


Figure 4. (a) Alfvén continuum spectrum for the $n = 2$ mode, safety factor profile with $q_0 \approx 1.4$ and measured TAE frequency (dashed line) at 4.8 s in the discharge shown in Fig. 2. (b) Similar spectrum for the assumed q profile with $q_0 = 1.2$.

calculated for the assumed q profile with $q_0 = 1.2$. Figure 4(b) shows the spectrum, the q profile and the measured TAE frequency. The TAE frequency intersects the Alfvén continuum spectrum because a new TAE gap is created at $r/a \approx 1.6$, which is the location of $q = 1.25$. It indicates that the TAE can be stable owing to the misalignment of the TAE gap. The effect of a small change in q_0 , from 1.4 to 1.2, on the fast ion pressure profile is insignificant. The relation between the Alfvén continuum spectrum and the measured frequency for different q profiles suggests that the stability is sensitive to q_0 and the tendency of TAE excitation only in the low ℓ_i regime can be understood from decreasing q_0 .

4. Burst modes and chirping modes

New burst modes and chirping modes (the mode with large frequency changes) were found in a high β regime of $\langle \beta_h \rangle \geq 0.2\%$. Figure 5 shows a typical

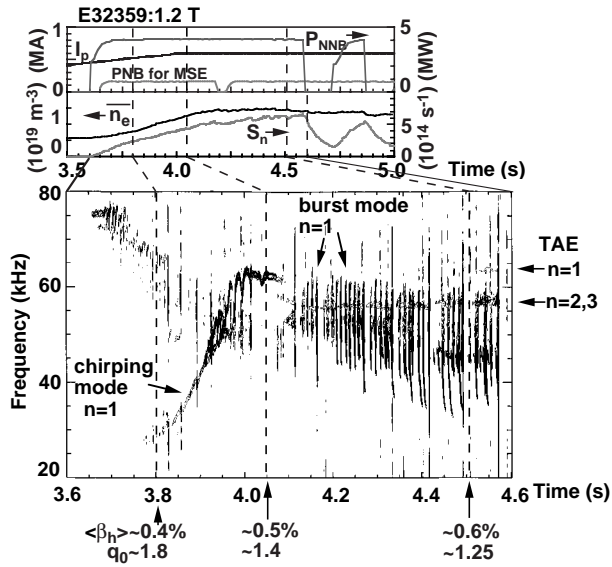


Figure 5. Top: time traces of plasma current I_p , NNB power P_{NNB} for MSE diagnostics, line averaged electron density \bar{n}_e and neutron emission rate S_n . Bottom: frequency spectrum of magnetic fluctuations measured during D⁰ NNB injection into a deuterium plasma. The beam energy is 360 keV and the toroidal magnetic field at the centre is 1.2 T. Toroidal mode numbers are shown for some typical modes.

discharge where burst modes and chirping modes have been observed simultaneously with TAEs and EAEs (ellipticity induced Alfvén eigenmodes). The top part of Fig. 5 shows the temporal behaviour of plasma current I_p , the beam power P_{NNB} for MSE diagnostics, the line averaged electron density \bar{n}_e and the neutron emission rate S_n . A D⁰ NNB of 360 keV was injected with a power of 4 MW into a deuterium plasma. The central magnetic field was 1.2 T. The ratio $v_{b\parallel}/v_A$ increased to 0.95 with electron density. Here, the slowing down time of NNB ions, τ_s , was ~ 0.3 s. The frequency spectrum of magnetic fluctuations is shown in the bottom part of the figure. Burst modes start ~ 0.1 s after the start of NNB injection, but the activity is weak. When the fast ion β increases and the safety factor at the centre decreases, the activity of the burst mode becomes strong. The volume averaged β of NNB ions is $\langle \beta_h \rangle \approx 0.5\%$ and $q_0 \approx 1.4$ at 4.05 s. The mode clearly seen for 4.1–4.57 s in the range 57–58 kHz is the $n = 2$ TAE; weak TAEs with $n = 1-3$ are detected in the range 60–70 kHz, though they are not clear in the frequency spectrum.

Figure 6 expands the 100 ms from 4.2 to 4.3 s during the appearance of burst modes in Fig. 5. The

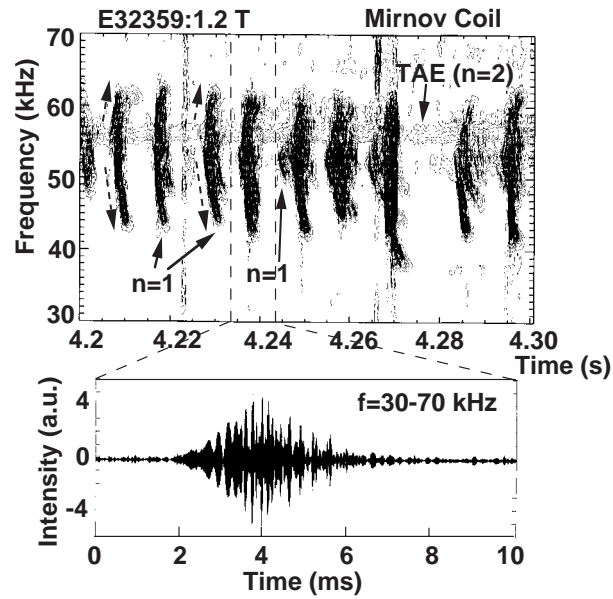


Figure 6. Top: expansion of the 100 ms from 4.2 to 4.3 s during the appearance of burst modes in Fig. 5. Toroidal mode numbers n are shown for typical modes. The directions of frequency change for upward and downward frequency branches are indicated with arrows. Bottom: time trace of magnetic fluctuations of a single burst.

time trace of magnetic fluctuations of a single burst is shown in the bottom part of the figure. The magnetic fluctuations are very similar to those of fish-bone instabilities. The burst mode occurs in a few milliseconds with ~ 10 ms interval. The mode frequency starting at around the $n = 2$ TAE changes rapidly (~ 20 kHz) during the burst. The burst mode frequencies are in the range $\omega \leq \omega_{TAE}$ and are much larger than the diamagnetic drift frequency of bulk ions of ~ 1 kHz. Two branches can be observed: the mode frequency decreases in one branch but increases in the other. The toroidal mode number of the burst modes is $n = 1$, as shown in Fig. 6.

The pressure profile of NNB ions was modified by selecting one of the two beam lines shown in Fig. 1. The pressure profiles calculated with the OFMC code are shown in Fig. 7. A strongly peaked pressure profile of NNB ions was obtained with the upper beam line and a hollow profile was produced with the lower beam line. In the range $r/a \geq 0.4$, the pressure is almost the same. The burst modes are strong for the peaked pressure profile but very weak for the hollow pressure profile. Therefore, the high pressure or the high pressure gradient of fast ions in the central region, or both are considered to be responsible for the burst mode excitation.

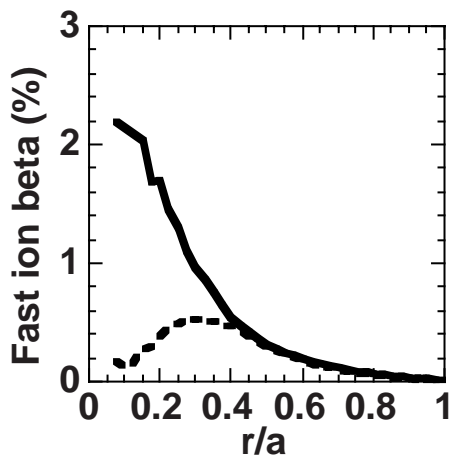


Figure 7. Profiles of fast ion β when only the upper beam line is used (solid line) and only the lower beam line is used (dashed line).

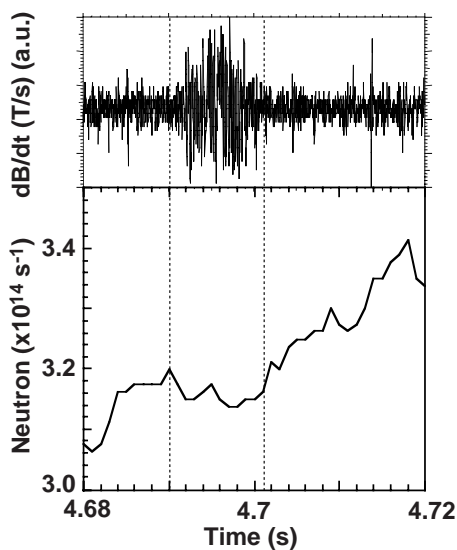


Figure 8. Temporal behaviour of magnetic fluctuations (top) and neutron emission rate (bottom) when a burst mode appears.

Figure 8 shows the temporal behaviour of magnetic fluctuations and the neutron emission rate when a burst mode appears. The amplitude of magnetic fluctuations of the burst modes is typically a few to ten times as large as that of TAEs and EAEs. A 2–3% drop in the neutron emission rate is induced by the burst modes. This small drop indicates that the loss of co-injected NNB ions is small. On the other hand, fast ion loss correlating with TAEs and EAEs is not clearly observed owing to the weak fast ion drive used so far.

Strongly chirping modes of $n = 1$ were detected during 3.8–4.1 s in the discharge shown in Fig. 5. The frequency chirping starts at ~ 30 kHz and the frequency increases to the TAE frequency range. A comparison between the Alfvén continuum for the $n = 1$ mode and the measured mode frequency at 3.8 s and at 4.05 s has shown that the measured frequency is well inside the Alfvén continuum at the start of chirp and is in the TAE gap at the end of chirp. This chirping phenomenon is similar to that observed in the ICRF heating of weakly reversed shear plasmas in JT-60U [10]. The large frequency chirping in Fig. 5 can be observed only in a time approximately equal to τ_s after the start of the NNB injection, where the bump on tail is formed.

5. Stabilization of Alfvén eigenmodes in strongly reversed shear plasmas

It has been found that a reversed shear plasma with internal transport barrier (ITB) is immune to TAEs driven by energetic ions produced with ICRF heating [9, 10, 21]. The TAEs have been observed only in weakly reversed shear plasmas with moderate ITB formed after sequential collapses. In recent experiments, the excitation and stabilization of TAEs in reversed shear plasmas were investigated by injecting NNBs into deuterium plasmas with $B_{t0} = 2.1$ T.

Figure 9 shows profiles of the safety factor, electron density and fast ion β of NNB ions in the case without exciting AEs. The q profile has a minimum (q_{min}) at $r/a \approx 0.7$ – 0.8 and is strongly reversed inside the location of q_{min} . Because of the ITB formation in the electron density, a slight jump in the density profile is observed just inside the location of q_{min} . The β_h profile shows that most of the NNB ions are deposited inside the ITB. The volume averaged fast ion β , $\langle \beta_h \rangle = 0.28\%$, is sufficiently higher than the threshold value, $\langle \beta_h \rangle \approx 0.1\%$, for TAE excitation. However, the fast ion β is low and the pressure gradient is small in the low shear region around q_{min} . The misalignment between the AE gap and a region of high pressure and large pressure gradient of NNB ions is considered to be the cause of the stabilization of AEs in the strongly reversed shear plasma.

On the other hand, the $n = 1$ TAE was observed in the weakly reversed shear plasma, as shown in Fig. 10(a). Profiles of q , n_e and β_h are presented in Fig. 10(b). The location of q_{min} is at $r/a \approx 0.6$ and the ITB in the electron density can be seen at around

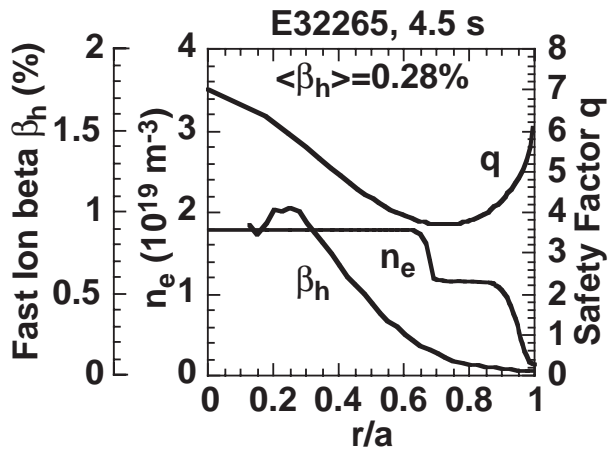


Figure 9. Profiles of safety factor q , electron density n_e and fast ion β , β_h , in a strongly reversed shear plasma with NNB injection in the case without exciting AEs.

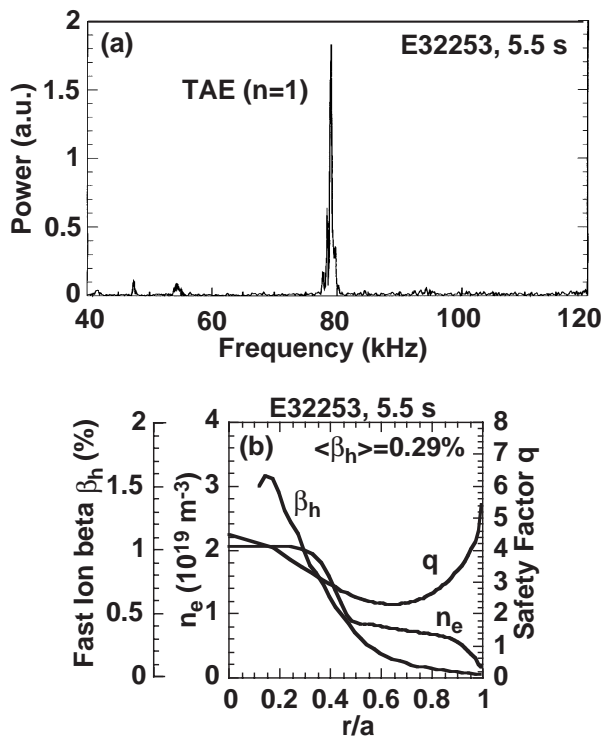
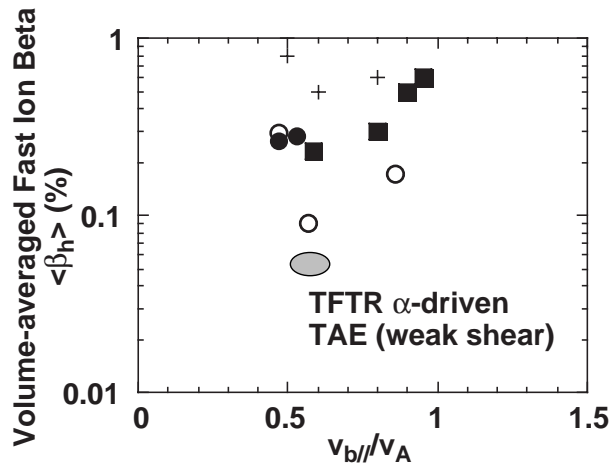


Figure 10. (a) Frequency spectrum of TAE observed in a weakly reversed shear plasma. (b) Profiles of safety factor q , electron density n_e and fast ion β , β_h , when the TAE was detected.

$r/a \approx 0.4-0.5$. The pressure profile of NNB ions is similar to that in the case of AE stabilization except for $r/a \leq 0.3$. The relation between the Alfvén



- JT-60U (weak and negative shear)**
- AEs (TAEs, EAEs)
 - No AE in R/S
 - burst mode + AEs
 - + DIII-D (positive shear)

Figure 11. A domain where AEs and burst modes have been observed in JT-60U is compared with the onset condition of weak AEs in positive shear plasmas on DIII-D [19] and with a domain of alpha particle driven TAEs in weak shear plasmas on TFTR [8].

continuum and measured TAE frequency indicates that the $n = 1$ TAE is excited in the TAE gap formed at $r/a \approx 0.5$, where magnetic shear is weak and the fast ion β is as high as $\sim 0.5\%$. The TAE is excited because of the well aligned TAE gap.

The condition for excitation of AEs and burst modes by NNB injection in JT-60U is plotted in a graph of $\langle \beta_h \rangle$ against $v_{b||}/v_A$ in Fig. 11 and compared with the onset condition of weak AEs in positive shear plasmas on DIII-D [19] and a domain where alpha particle driven TAEs have been excited in weak shear plasmas on TFTR [8]. The TAE starts to be excited at $\langle \beta_h \rangle \approx 0.1\%$ in the weak shear plasma and the β value is comparable to the threshold for TAE excitation by alpha particles in TFTR weak shear plasma. In a regime of $\langle \beta_h \rangle \geq 0.2\%$, burst modes are excited in addition to TAEs and EAEs. The TAE is also excited for $\langle \beta_h \rangle \approx 0.3\%$ in a weakly reversed shear plasma, but TAEs become stable in strongly reversed shear plasmas with similar β value. The figure also shows that not only macroscopic parameters such as $\langle \beta_h \rangle$ but also local parameters such as magnetic shear and pressure gradient of hot ions

are important for understanding AE excitation and stabilization.

6. Summary

The excitation and stabilization of AEs in weak or reversed magnetic shear plasmas were investigated with NNB injection at 330–360 keV. The TAEs were observed in weak shear plasmas with $\langle\beta_h\rangle \geq 0.1\%$ and $0.4 \leq v_{b\parallel}/v_A \leq 1$. The threshold $\langle\beta_h\rangle \approx 0.1\%$ is as low as the threshold β_α in weak shear TFTR discharges. The TAEs are stable in the high ℓ_i regime of $\ell_i \geq 1$ for $\langle\beta_h\rangle \approx 0.1\%$. The excitation and stabilization are consistent with predictions by the NOVA-K code. New burst modes and chirping modes were observed at a higher β of $\langle\beta_h\rangle \geq 0.2\%$. A burst mode occurs in the range $\omega \leq \omega_{TAE}$ and the mode frequency changes rapidly by ~ 20 kHz in a burst of a few milliseconds. The amplitude of the burst modes is a few times to ten times as large as that of TAEs and EAEs at the plasma edge. A drop in the neutron emission rate by a few per cent was observed to correlate with the burst modes. Fast ion loss correlating with TAEs and EAEs was not clearly observed owing to the weak fast ion drive. The chirping modes appear in an early phase of the NNB injection and the mode frequency starts to chirp from inside the Alfvén continuum and increases to the TAE frequency. These chirping modes are excited only in a duration as long as the slowing down time of NNB ions after the start of NNB injection. In the strongly reversed shear plasma with the ITB, AEs were suppressed. This is considered to be due to the misalignment of the AE gap and/or the low pressure gradient and low fast ion β in the low shear region.

Acknowledgements

The authors would like to thank their colleagues at the Japan Atomic Energy Research Institute who have contributed to the JT-60 project. The authors would like to express their appreciation to H. Kishimoto, M. Azumi and A. Funahashi of JAERI and to R.J. Goldston and K. Young of the Princeton Plasma Physics Laboratory for their strong support of the collaboration between the two institutions.

References

- [1] Ozeki, T., et al., in Plasma Physics and Controlled Nuclear Fusion Research 1992 (Proc. 14th Int. Conf. Würzburg, 1992), Vol. 2, IAEA, Vienna (1993) 187.
- [2] Cheng, C.Z., Chen, L., Chance, M.S., Ann. Phys. (N.Y.) **161** (1984) 21.
- [3] Cheng, C.Z., Chance, M.S., Phys. Fluids **29** (1986) 3695.
- [4] Wong, K.L., et al., Phys. Rev. Lett. **66** (1991) 1874.
- [5] Fu, G.Y., et al., Phys. Rev. Lett. **75** (1995) 233.
- [6] Fu, G.Y., et al., Phys. Plasmas **3** (1996) 4036.
- [7] Nazikian, R., et al., in Fusion Energy 1996 (Proc. 16th Int. Conf. Montreal, 1996), Vol. 1, IAEA, Vienna (1997) 281.
- [8] Nazikian, R., et al., Phys. Rev. Lett. **78** (1997) 2976.
- [9] Kimura, H., et al., in Fusion Energy 1996 (Proc. 16th Int. Conf. Montreal, 1996), Vol. 3, IAEA, Vienna (1997) 295.
- [10] Kusama, Y., et al., Nucl. Fusion **38** (1998) 1215.
- [11] Ushigusa, K., JT-60 Team, in Fusion Energy 1996 (Proc. 16th Int. Conf. Montreal, 1996), Vol. 1, IAEA, Vienna (1997) 37.
- [12] Kuriyama, M., et al., in Proc. 17th IEEE/NPSS Symp. on Fusion Engineering, San Diego, CA, 1997.
- [13] Fujita, T., et al., in Fusion Energy 1996 (Proc. 16th Int. Conf. Montreal, 1996), Vol. 1, IAEA, Vienna (1997) 227.
- [14] Fujita, T., et al., Phys. Rev. Lett. **78** (1997) 2377.
- [15] Ishida, S., et al., Phys. Rev. Lett. **79** (1997) 3917.
- [16] Fujita, T., Kubo, H., Sugie, H., Isei, N., Ushigusa, K., Fusion Eng. Des. **34–35** (1997) 289.
- [17] Tani, K., Azumi, M., Kishimoto, H., Tamura, S., J. Phys. Soc. Jpn. **50** (1981) 1726.
- [18] Strait, E.J., et al., Nucl. Fusion **33** (1993) 1849.
- [19] Heidbrink, W.W., Plasma Phys. Control. Fusion **37** (1995) 937.
- [20] Heidbrink, W.W., Strait, E.J., Doyle, E., Sager, G., Snider, R.T., Nucl. Fusion **31** (1991) 1635.
- [21] Ozeki, T., et al., Plasma Phys. Control Fusion **39** (1997) A371.

(Manuscript received 9 December 1998
Final manuscript accepted 6 April 1999)

E-mail address of Y. Kusama:
kusama@naka.jaeri.go.jp

Subject classification: D2, Te; D2, Ti